ELSEVIER

Journal of Nuclear Materials 250 (1997) 236–241

journal of nuclear materials

Damage region formation in ferritic steels induced by light water reactor neutron spectrum

P.V. Vladimirov [a], A.I. Ryazanov [a,*], Yu.D. Lizunov [a], J.C. Van Duysen [b]

[a] *RRC 'Kurchatov Institute', 123182 Moscow, Russia*

[b] *Electricité de France, Departement Etude des Materiaux, Les Renardieres route de Sens, BP 1, Ecuelles, 77250 Moret sur Loing, France*

Received 11 September 1996; accepted 10 June 1997

Abstract

A new theoretical model for damage region formation is proposed. The model is based on numerical solution of the Boltzmann transport equation for knocked-on atoms. A key point of this model is the selfconsistent determination of subcascade overlapping energy E_{over} (the threshold energy for distinguished damage region formation). Damage region density and size distributions in ferritic steels (Fe–0.2 wt% Cu and Fe–0.2 wt% Cu–0.3 wt% Si) under neutron irradiation in light water reactor spectrum were calculated. © 1997 Elsevier Science B.V.

1. Introduction

The investigation of collisional cascade spatial structure presents a difficult problem to study by either theoretical or experimental means. All existing experimental techniques are limited to indirect measurements of cascade manifestation. On the contrary there are at least three theoretical methods of collisional cascade investigation. The binary collision approximation (BCA) [1–3] allows simulation of high energy collision cascades. BCA is valid only for collisions above a few eV. The molecular dynamics method (MDM) [4–6] is able to treat cascade formation in the low energy range and is used extensively for simulation of defect annealing in the cascade zone. These methods give an opportunity to investigate in cascade defect cluster formation, recombination of the point defects depending on the cascade zone cooling rate, the process of cascade breakup into subcascades and many other cascade features. Methods based on the solution of the linearized Boltzmann transport equation [7–9] have approximately the same region of validity as BCA and have not been used before for the studies of collisional cascade structure.

The configuration of high energy cascade is very irregular and it is difficult to distinguish individual subcascades. The other difficulty is an absence of the obvious conditions under which the breakup into subcascades occurs.

In the present paper damage region structure in the ferritic steels (Fe–0.2 wt% Cu and Fe–0.2 wt% Cu–0.3 wt% Si) formed under neutron irradiation will be studied using the direct solution of Boltzman transport equation for knocked-on atoms.

2. Subcascade formation

We follow the threshold model of subcascade formation suggested in [10,11] with some modifications. In order to describe the process of subcascade formation we will track movement of primary knocked-on atom (PKA) between collisions resulting in subcascade formation.

The subcascade size can be estimated as a range of secondary knocked-on atom (SKA). Energy of SKA depends on PKA energy and differential scattering cross-section. Therefore SKAs possess their own energy distribution in reality. In spite of this fact we will assume that SKA energy is fixed and is choused to be equal to the average value over SKA energy spectrum. According to this assumption subcascade size is also fixed and depends only on PKA energy.

* Corresponding author.

PII S0022-3115(97)00211-0

Distance between collisions with subcascade creation is controlled by total elastic cross-section of PKA scattering on lattice atoms. The distance is a small part of the total PKA range. Hence, energy loss between subcascade creating collisions can be neglected. Each subcascade is taken to be a sphere and it is supposed that subcascades are not overlapped, when distance between centers of subcascades is greater than subcascade diameter. The value of PKA energy E_{over} corresponding to touching of subcascade spheres will be called subcascade overlapping energy.

It means that PKAs with energy $E_{\text{PKA}} < E_{\text{over}}$ will produce overlapped subcascades, and for $E_{\text{PKA}} > E_{\text{over}}$ subcascades are not overlapped. Here and after we will term overlapped subcascades as damage region.

In order to obtain threshold energy for cascade overlapping E_{over} let us compare the distance between collisions of primary knocked-on atom (PKA) and the subcascade size. At high energies the distance between collisions of PKA with atoms λ can be larger than the subcascade size R_{c} In this case the damaged zone is divided into distinguishable subcascades. The distance between collisions of PKA is determined by the elastic scattering cross-section $\sigma_{kl}(E, T)$ for transfer to l-type target atom more energy than T from k-type PKA with kinetic energy E:

$$\lambda_{kl}(E, T) = \frac{1}{N_l \sigma_{kl}(E, T)}, \tag{1}$$

where N_l is l-type atomic density and the cross-section $\sigma_{kl}(E, T)$ is defined by

$$\sigma_{kl}(E, T) = \int_T^{T_{\max}^{kl}} \mathrm{d}T' \frac{\mathrm{d}\sigma_{kl}(E, T')}{\mathrm{d}T'}. \tag{2}$$

Here $(\mathrm{d}\sigma_{kl}(E, T))/(\mathrm{d}T)$ is the differential cross-section of energy transfer T from k-type PKA with energy E to l-type target atom, $T_{\max}^{kl}$ maximum energy transfer in such collision. The transferred to SKA energy T should be high enough to produce a subcascade and will be determined later.

The subcascade size R_{c} can be estimated as a range of secondary knocked-on target atom (SKA), with energy taken to be equal to the average energy transfer $\bar{T}_{\text{SKA}}$ from PKA to SKA:

$$\bar{T}_{\text{SKA}}^{kl}(E_{\text{PKA}}) = \frac{1}{\sigma_{tot}^{kl}} \int_{E_{\text{d}}^l}^{T_{\max}^{kl}} \mathrm{d}T \frac{\mathrm{d}\sigma^{kl}(E_{\text{PKA}}, T)}{\mathrm{d}T} T, \tag{3}$$

where E_{d}^l is the threshold energy of displacement for l-type atom, and σ_{tot}^{kl} is the corresponding total elastic cross-section.

Therefore the size of subcascade R_{c}^{kl} formed by l-type SKA, knocked-on by k-type PKA, can be written as

$$R_{\text{c}}^{kl} = R_l\left(\bar{T}_{\text{SKA}}^{kl}\right) = \int_0^{\bar{T}_{\text{SKA}}^{kl}} \frac{\mathrm{d}E'}{S_{\text{tot}}^l(E')}, \tag{4}$$

$$S_{\text{tot}}^l(E) = S_{\text{n}}^l(E) + S_{\text{e}}^l(E), \tag{5}$$

where $S_{\text{n}}^l(E)$, $S_{\text{e}}^l(E)$ are the nuclear and electronic stopping power for l-type SKA respectively.

It should be emphasized that the obtained dependence of the subcascade size R_{c}^{kl} on PKA energy is completely different from common range — energy dependence $R_l(E)$. This dependence can be written in the form of composition of two functions: $R_{\text{c}}^{kl}(E_{\text{PKA}}) = R_l(\bar{T}_{\text{SKA}}^{kl}(E_{\text{PKA}}))$.

The criterion of subcascade overlapping is based on the comparison of the distance between cascade creating collisions of PKA and the size of subcascade. It gives us the minimum critical PKA energy E_{over} for subcascades overlapping:

$$R_{kl}(E_{\text{over}}) = R_l\left(\bar{T}_{\text{SKA}}^{kl}(E_{\text{over}})\right) = \lambda_{kl}(E_{\text{over}}, T). \tag{6}$$

The usage of the relation will be discussed later in Section 5.

3. Knocked-on atom transport calculations

Fast neutrons produce displacement damage homogeneously over the specimen volume. So the space and time independent form of Boltzman transport equation for knocked-on atoms can be used for description of atomic collision cascades under fast neutron irradiation:

$$-\frac{\mathrm{d}}{\mathrm{d}E}\left[S_{\text{e}}^k(E)\Phi_k(\vec{\Omega}, E)\right] = I_k + q_k(\vec{\Omega}, E). \tag{7}$$

Here $\Phi_k(\vec{\Omega}, E)$ is the scalar k-type atom flux, $S_{\text{e}}^k(E) = -\mathrm{d}E_{\text{k}}/\mathrm{d}x$ — the electronic stopping power for k-type atoms; $q_{\text{k}}(\vec{\Omega}, E)$ is the density of the external source of k-type primary knocked-on atoms induced by fast neutron irradiation with given energy spectrum; I_k is the collision integral, which in our case can be written:

$$\begin{aligned} I_k = & \sum_i N_i \int \mathrm{d}\sigma_{ki}\left(E', \vec{\Omega}' \to E, \vec{\Omega}; \vec{\Omega}''\right)\Phi_k \\ & \times(\vec{\Omega}', E')\,\mathrm{d}E'\,\mathrm{d}\vec{\Omega}' - \sum_i N_i \Phi_k(\vec{\Omega}, E) \\ & \times \int \mathrm{d}\sigma_{ki}\left(E, \vec{\Omega} \to E', \vec{\Omega}'; \vec{\Omega}''\right)\mathrm{d}E'\,\mathrm{d}\vec{\Omega}' \\ & + N_k \sum_i \int \mathrm{d}\sigma_{ik}\left(E', \vec{\Omega}' \to E'\right. \\ & \left. -E, \vec{\Omega}''; \vec{\Omega}\right)\Phi_k(\vec{\Omega}', E')\,\mathrm{d}E'\,\mathrm{d}\vec{\Omega}'. \end{aligned} \tag{8}$$

Here N_k stands for the atomic density of k-type atoms in the target, $\mathrm{d}\sigma_{ki}(E, \vec{\Omega}' \to E', \vec{\Omega}'; \vec{\Omega}'')$ is the differential cross-section of k-type moving atom collisions with i-type target atoms. E and $\vec{\Omega}$ are the initial energy and velocity direction of incident k-type atom, whereas E' and $\vec{\Omega}'$ are the same values after collision and $\vec{\Omega}''$ stands for the direction of the i-type recoil atom movement.

The first term in Eq. (8) describes the atoms coming to the phase space domain near the point $(\vec{\Omega}, E)$. The second one stands for the atom leaving this domain due to collisions. The third term describes moving atom generation due to elastic collisions.

For the present calculations we use Kinchin–Pease type threshold energy model for single cascade generation [12] to estimate a number of subcascades. The code was modified to calculate the flux of moving atoms crossing the plane $E = E_{\text{over}}$ in phase space. The number of such atoms gives us the number of distinguished damage regions, and the energy distribution $\Xi_{\text{k}}(E)$ for k-type atoms together with energy dependence of range $R_{\text{k}}(E)$ can be used to calculate the size distribution of damage regions $\Xi_{\text{k}}(R_{\text{k}})$ The flux of moving atoms crossing the plane $E = E_{\text{over}}$ consists of two parts, one is due to continuous slowing down and the other is due to collisional 'jumps' and can be expressed in terms of k-type atom scalar flux $\Phi_{\text{k}}(\vec{\Omega}, E)$:

$$\Xi_k(E) = \left\{ \frac{\mathrm{d}}{\mathrm{d}E} \left[S_{\text{e}}^k(E) \int_{4\pi} \mathrm{d}\vec{\Omega}\, \Phi_k(\vec{\Omega}, E) \right] \right\} \Bigg|_{E = E_{\text{over}}^k} + \sum_i \int_{E > E_{\text{over}}^i} \mathrm{d}E'' \int_{4\pi} \mathrm{d}\vec{\Omega}\, N_k \int \mathrm{d}\sigma_{ik}\left(E', \vec{\Omega}' \to E'', \vec{\Omega}\right) \Phi_i(\vec{\Omega}', E')\, \mathrm{d}E'\, \mathrm{d}\vec{\Omega}'. \tag{9}$$

The whole energy interval is defined as follows:

$$E_0 \geq E \geq \min_i \left(E_{\text{over}}^i \right) = E_{\min},$$

where E_0 stands for the maximal source energy. The physical parameters necessary for solution of Eq. (7) are $S_{\text{e}}^k(E)$ and differential cross-section of interatomic collisions $\mathrm{d}\sigma_{ki}$.

In accordance with Ref. [13] we shall assume that the inelastic energy loss of moving ion is fully determined by it's interaction with the electronic subsystem of the target and is described by $S_k(E)$. So we shall treat the collisions with significant changes of ion direction as elastic.

Following Lindhard [13,14] we will treat the differential cross-section, which depends on two values: the impact ion energy E and the recoil atom energy T, as a function of one variable t:

$$t = TE \frac{M_{\text{a}}}{M_{\text{i}}} \left(\frac{a}{2 Z_{\text{a}} Z_{\text{i}} e^2} \right), \tag{10}$$

where M_{a}, Z_{a}, M_{i} and Z_{i} are the incident ion and the target atom masses and charges respectively, e is the electron charge and

$$a = 0.8853 a_{\text{b}} \left(Z_{\text{a}}^{2/3} + Z_{\text{i}}^{2/3} \right)^{-1/2}, \tag{11}$$

with $a_{\text{b}} = 0.53 \times 10^{-8}$ cm. Thus the differential cross-section can be written as

$$\mathrm{d}\sigma = \pi a^2 \frac{\mathrm{d}t}{2t^{3/2}} f(t^{1/2}). \tag{12}$$

Here $f(t^{1/2})$ is determined by the actual interatomic potential. For the Thomas–Fermi atom model $f(t^{1/2})$ was obtained numerically in [13].

Another value needed for the solution of Eq. (7) is the electronic stopping power function $S_{\text{e}}^k(E)$. It characterizes the mean energy loss of a moving atom on a unit path length due to interaction with the electronic subsystem of a target.

No theory gives a unique description of $S_{\text{e}}(E)$ in the whole energy range. For low ion energies $(v < v_{\text{b}} Z_{\text{a}}) S_{\text{e}}(E)$ is proportional to the velocity of a moving atom: $S_{\text{e}}(E) \propto E^{1/2}$ [15].

One can use the Bethe–Bloch theory [16,17] at very high energies which leads to: $S_{\text{e}}(E) \propto (1/E)\ln(E)$.

In the intermediate energy region we interpolate $S_{\text{e}}(E)$ as

$$S_{\text{e}} = \left(S_{\text{low}}(E)^{-1} + S_{\text{high}}(E)^{-1} \right)^{-1}. \tag{13}$$

For compound targets, Bragg's additivity rule for $S(E)$ calculations was used.

Solution of Eq. (7) was performed by means of using computer code BOLT, which was described in details for a more general case of ion irradiation in [18]. The BOLT code was also modified to accept the source of PKA with complicated energy spectrum induced by fast neutron irradiation.

4. Neutron induced PKA spectrum

Radiation damage calculations involve determination of primary recoil spectrum (PRS) induced by neutron irradiation. The PRS depends on the neutron scattering cross-section and the neutron spectrum. The number of i-type PKA per unit energy is defined as

$$q_i(T) = \int \mathrm{d}E_{\text{n}}\, \Phi(E_{\text{n}}) \sum_r N_i \sigma_i^{\text{r}}(E_{\text{n}}, T), \tag{14}$$

where $\Phi(E_{\text{n}})$ is the differential energy spectrum of neutrons, and $\sigma_i^{\text{r}}(E_{\text{n}}, T)$ is the differential cross-section of the energy transfer T to the i-type recoil from neutron with energy E in nuclear channel r. We use these spectra as a source in Eq. (7) for the displacement damage and cascade size calculations.

Neutron cross-sections for different kinds of nuclei as well as energy and angular distributions of scattered neutrons are available in different evaluated nuclear data files. In the present work we have used ENDF-6 library in ENDF/B-VI format. The NJOY code [19] was used for multigroup PKA spectra calculations. Only elastic and discrete inelastic reactions were considered. For these nuclear channels the recoil atom energy is fully determined by energy and momentum conservation laws.

Damage and subcascade generation rates are the main parameters of radiation damage. These values can be calculated using the total number of j-type atoms $\nu_{ij}(T)$ knocked-on by i-type PKA with energy T, which will be determined from the numerical solution of Boltzman transport Eq. (7).

If partial values $\nu_{ij}(T)$ are known, the displacement damage $G_{\rm d}^j$ and subcascade $G_{\rm c}^j$ generation rates of j-type atoms can be written as

$$G_{\rm d}^j = \sum_i \int_{E_d^j}^{T_{\rm m}^{ij}} {\rm d}T q_i(T) \nu_{ij}(T), \tag{15}$$

$$G_{\rm c}^j = \sum_i \int_{E_{\rm over}^i}^{T_{\rm m}^{ij}} {\rm d}T q_i(T) \nu_{ij}(T). \tag{16}$$

The values of $G_{\rm d}^j$ and $G_{\rm c}^j$ were calculated using the solution of Boltzman transport Eqs. (7) and (8) by direct count of the displaced atom number with energies $E > E_{\rm d}^j$ and $E > E_{\rm over}$ respectively.

5. Results

Size of damage region $R_{\rm c}^{kl}(E_{\rm PKA}) = R_l(\bar{T}_{\rm SKA}^{kl}(E_{\rm PKA}))$ and distance between subcascades as a function of PKA energy are presented at Fig. 1. We can see that at transfer energy $T = 0.5$ keV curves for the subcascade size and distance between collisions for silicon do not intersect. It means that in this case subcascades are formed along the trajectory of PKA and they are not overlapping. At transfer energy $T = 0.1$ keV situation changes and these curves intersect. In this case, the structure of the damage zone is

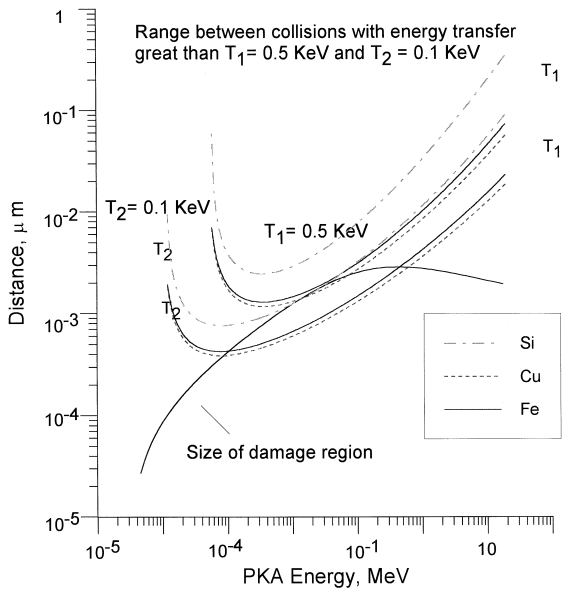

Fig. 1. Subcascade size and the distance between subcascades vs. primary knocked-on atom energy.

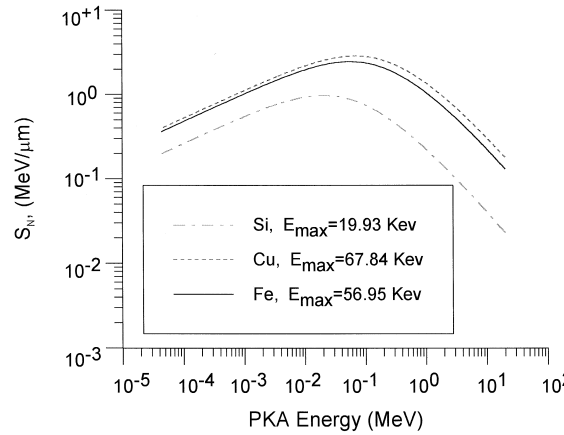

Fig. 2. Nuclear stopping power of Si, Fe and Cu in ferritic steel (Fe–0.2 wt% Cu–0.3 wt% Si).

different. Subcascades are overlapped and damage region is determined by cascade size. If we proceed from higher transfer energy to lower, we can encounter that at some critical value $T_{\rm cr}$ these curves begin to touch on. We will determine threshold subcascade overlapping energy of PKA $E_{\rm over}$ just for this critical value of transfer energy $T_{\rm cr}$. It can be seen from the Fig. 1 that values of subcascade overlapping energy $E_{\rm over}$ for different components (Si, Cu, Fe) of ferritic steels are not so different. It is interesting to compare the overlapping energy $E_{\rm over}$ with PKA energy corresponding to maximum of nuclear stopping power $E_{\rm max}$. The intensive generation of cascades occurred at this energy. Nuclear stopping powers of silicon, iron and copper ions slowing down in ferritic steel are presented on Fig. 2. It is interesting to note that the overlapping energy $E_{\rm over}$ and energy of maximum of nuclear stopping power $E_{\rm max}$ have the same order, but $E_{\rm over}$ is less than $E_{\rm max}$.

We will calculate the subcascade generation rate for ferritic steels using neutron spectrum of light water nuclear reactor. This neutron group flux is presented on Fig. 3.

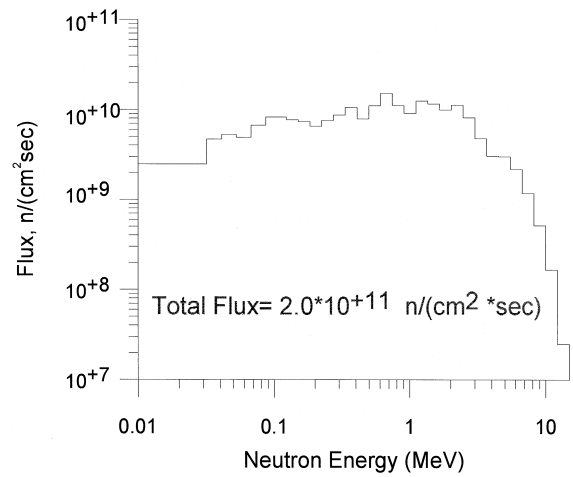

Fig. 3. Group neutron flux for light water reactor.

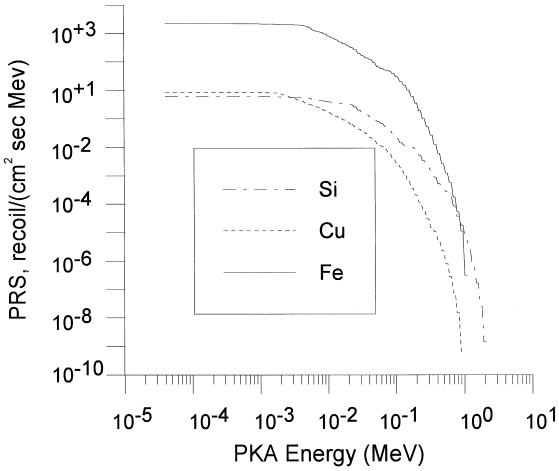

Fig. 4. Differential primary recoil atom spectra.

For the following calculations we have to know the primary knocked-on atom spectrum. Using the Eq. (14) and the neutron group flux presented on Fig. 3 we have calculated PRS for each component, which are shown on Fig. 4.

We have calculated number of subcascades as a function of PKA energy. Using this function and energy dependence of subcascade size we can obtain generation rate for subcascade density as a function of size. In order to investigate the effect of subcascade overlapping energy value on the damage region formation we performed calculation for three values of overlapping energy ($E_{over} = 5$, 10, 20 keV). These results for different components are presented on Figs. 5–7. It can be seen that generation rate for subcascades increases with subcascade size. Effective subcascade size is larger for higher E_{over} (compare Fig. 5 for $E_{over} = 20$ keV and Fig. 7 for $E_{over} = 5$ keV). Maximal generation rate of subcascades for these ferritic steels is realized on iron.

As an additional result the dependence of partial damage cross-sections on neutron energy were calculated. This

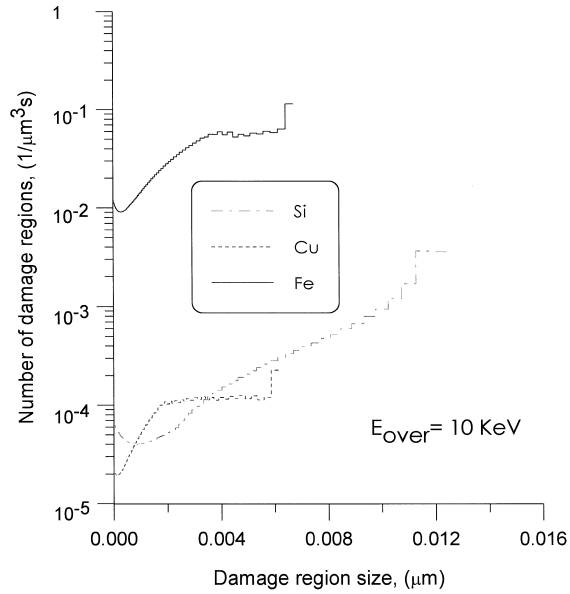

Fig. 6. Number of subcascades vs. subcascade size for $E_{over} = 10$ keV.

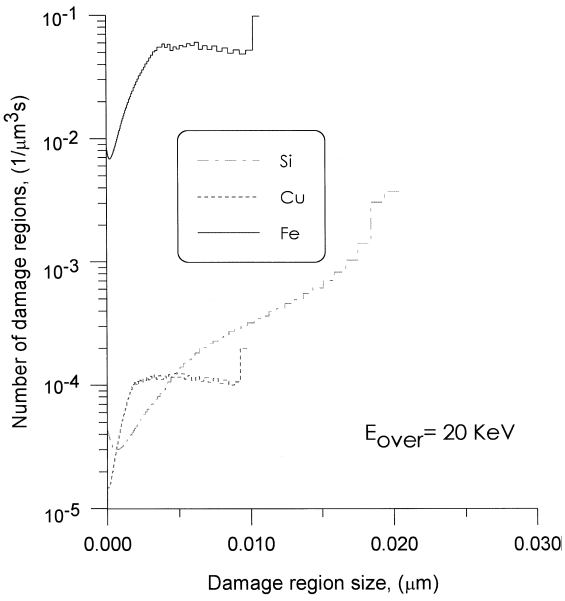

Fig. 5. Number of subcascades vs. subcascade size for $E_{over} = 20$ keV.

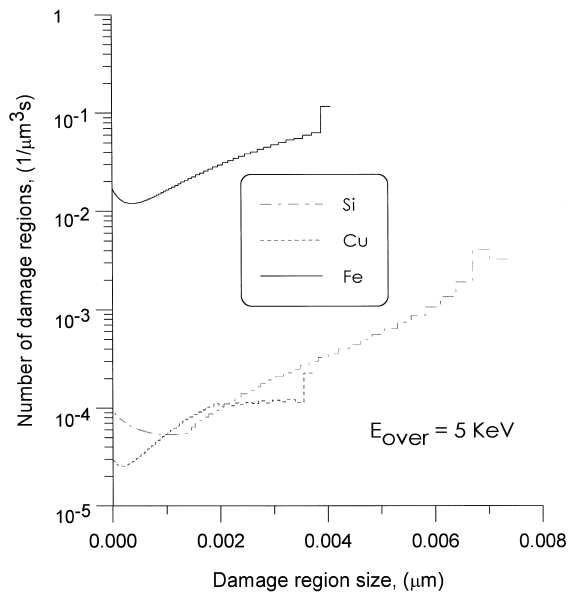

Fig. 7. Number of subcascades vs. subcascade size for $E_{over} = 5$ keV.

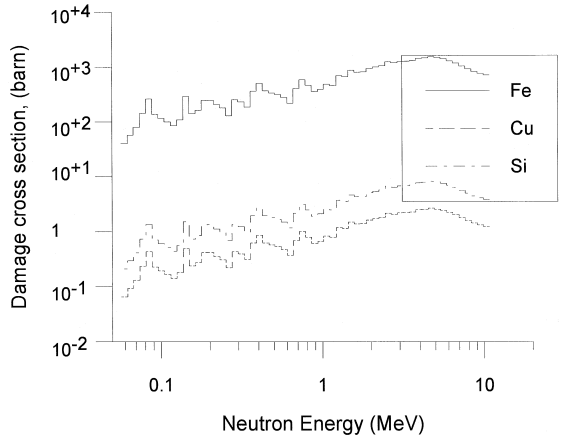

Fig. 8. Damage cross-sections vs. neutron energy for ferritic steel components

results are presented on Fig. 8. Total damage cross-sections are $\sigma_d = 36.3 \times 10^3$ barn for Fe, $\sigma_d = 61.9$ barn for Cu, $\sigma_d = 192.7$ barn for Si.

Damage generation rate of point defect has been also calculated for neutron group flux presented on Fig. 3. Calculations give the following values for partial damage generation rates $G_d = 1.0 \times 10^{-10}$ dpa/s for Fe, $G_d = 1.7 \times 10^{-13}$ dpa/s for Cu and $G_d = 5.3 \times 10^{-13}$ dpa/s for Si.

Subcascade generation rates per unit volume are equal to $G_c = 1.25 \times 10^{-3}$ subc/(μm^3 s) for Fe, $G_c = 3.08 \times 10^{-6}$ subc/(μm^3 s) for Cu, $G_c = 5.3 \times 10^{-5}$ subc/(μm^3 s) for Si.

6. Conclusions

Using the Boltzmann transport equation for knocked-on atoms allows us to investigate the problem of cascade breakup into subcascades. The key point of such calculations is the determination of subcascade overlapping energy, which can be determined from microscopical characteristics of atomic collisions and slowing down. Subcascade generation rate in ferritic steels was obtained as a function of damage region size for light water nuclear reactor neutron spectrum.

References

[1] M.T. Robinson, I.M. Torrens, Phys. Rev. B9 (1972) 5008.
[2] H.L. Heinisch, J. Nucl. Mater. 117 (1983) 47.
[3] H.L. Heinisch, J. Nucl. Mater. 103 (1981) 1325.
[4] A.J.E. Foreman, W.J. Phythian, C.A. English, The Molecular Dynamics Simulation of Irradiation Damage Cascades Using Many-Body Potentials, AEA Technology Report, AEA-TRS-2031, UKAEA, Harwell UK, 1991.
[5] T. Diaz de la Rubia, M.W. Guinan, Phys. Rev. Lett. 66 (1991) 2766.
[6] T. Diaz de la Rubia, M.W. Guinan, Mater. Sci. Forum 97–99 (1992) 23.
[7] P. Sigmund, Rev. Roum. Phys. 17 (1972) 823, 969.
[8] Yu.D. Lizunov, A.I. Ryazanov, Rad. Eff. 60 (1982) 95.
[9] Yu.D. Lizunov, A.I. Ryazanov, Poverkhnost 5 (1987) 121, (in Russian).
[10] Y. Satoh, S. Kojima, T. Yoshiie, M. Kiritani, J. Nucl. Mater. 179–181 (1991) 901–904.
[11] Y. Satoh, T. Yoshile, M. Kiritani, J. Nucl. Mater. 191–194 (1992) 1101.
[12] G.H. Kinchin, R.S. Pease, Rep. Prog. Phys. 18 (1955) 1.
[13] J. Lindhard, V. Nielsen, M. Scharff, P.V. Thomsen, Dan. Vid. Selsk. Mater. Fys. Medd. 33 (10) (1963) 1.
[14] J. Lindhard, V. Nielsen, M. Scharff, Dan. Vid. Selsk. Mater. Fys. Medd. 36 (10) (1968) 1.
[15] J. Lindhard, M. Scharff, Phys. Rev. 121 (1) (1961) 128.
[16] H. Bethe, Ann. Phys. 5 (1930) 325.
[17] F. Bloch, Ann. Phys. 16 (1933) 285.
[18] Yu.D. Lizunov, A.I. Ryazanov, Boltzman transport equation in ion transport and radiation damage calculations, preprint IAE-5298/11, Moscow, 1991.
[19] R.E. MacFarlane, D.W. Muir, R.M. Boicourt, The NJOY Nuclear Data Processing System, Vol I: User's Manual LA-9303-M, (ENDF-324), May 1982.